Global deficiency of stearoyl-CoA desaturase-2 protects against diet-induced adiposity

Lucas M. O'Neill[a], **Yar Xin Phang**[a], **Majaliwa Matango**[a], **Sohel Shamsuzzaman**[a], **Chang-An Guo**[a], **David W. Nelson**[b], **Chi-Liang E. Yen**[b], **James M. Ntambi**[a,b,*]

[a]Department of Biochemistry, University of Wisconsin-Madison, 433 Babcock Drive, Madison, WI, 53706, USA

[b]Department of Nutritional Sciences, University of Wisconsin-Madison, 1415 Linden Drive, Madison, WI, 53706, USA

Abstract

In mouse, there are four stearoyl-CoA desaturase isoforms (SCD1–4) that catalyze the synthesis of monounsaturated fatty acids. Previously, we have shown that mice harboring a whole body deletion of the SCD1 isoform (SCD1KO) are protected from diet and genetically induced adiposity. Here, we report that global deletion of the SCD2 isoform (SCD2KO) provides a similar protective effect against the onset of both high-fat diet (HFD) and high-carbohydrate diet (HCD) induced adiposity. After 10 weeks of HFD feeding or 6 weeks of HCD feeding, SCD2KO mice failed to gain weight and had decreased fat mass. On HFD, SCD2KO mice remained glucose and insulin tolerant. Lastly, the markers for energy expenditure, UCP1 and PGC-1α, were increased in the brown adipose tissue of HFD fed SCD2KO mice.

1. Introduction

Currently, the global obesity epidemic continues to grow leading to the increased prevalence of chronic metabolic diseases such as cardiovascular disease, type 2 diabetes, non-alcoholic fatty liver disease, and cancer [1]. Comprehensive investigations into the biochemical pathways that promote obesity can lead to new treatments for obesity and obesity related diseases. One biochemical pathway of interest is the *de novo* synthesis of monounsaturated fatty acids (MUFAs).

There are four stearoyl-CoA desaturase isoforms (SCD1–4) in mouse and two in human (hSCD1 and hSCD5) that catalyze the *de novo* synthesis of MUFAs from saturated fatty acid (SFA) precursors. SCD1, hSCD1, SCD2, and SCD4 catalyze the conversion of palmitoyl (16:0)-CoA and stearoyl (18:0)-CoA to palmitoleoyl (16:1n7)-CoA and oleoyl (18:1n9)-CoA, respectively. SCD3 predominantly converts (16:0)-CoA to (166:1n7)-CoA [2];

*Corresponding author. Department of Biochemistry, University of Wisconsin-Madison, 433 Babcock Drive, Madison, WI, 53706, USA. ntambi@biochem.wisc.edu (J.M. Ntambi).

whereas, hSCD5 predominantly converts (18:0)-CoA to (18:1n9)-CoA [3]. All SCD isoforms are integral proteins that are embedded in the endoplasmic reticulum [4]. The products of SCD are signaling molecules and major components of membrane phospholipids (PL), triglycerides (TG), cholesterol esters (CE), and wax esters [5–7].

Although all SCD isoforms share >70% nucleotide and amino acid sequence similarity, SCD1 and SCD2 are the most similar in sequence, substrate specificity, and tissue expression [2]. SCD1 is the most abundant isoform and is highly expressed in lipogenic tissues such as adipose and liver. SCD2 is expressed ubiquitously except in the adult liver and is the predominant isoform in brain [2,8]. SCD3 is found in the harderian gland, preputial gland, and sebocytes [9]. SCD4 is restricted to the heart [10]. hSCD5 shares a similar tissue expression patten to SCD2 and is the predominant isoform in the human brain [11,3].

Of the four murine SCD isoforms, SCD1 has been the most characterized. Loss of SCD1 is protective against HFD and HCD induced adiposity [12,13]. It is also a major regulator of whole body energy homeostasis and is a potential drug target for the treatment of metabolic syndrome, cancer, Alzheimer's disease, Parkinson's disease, and skin disorders [14–16]. On the other hand, SCD2 has been shown to be important for neonatal development and hypothalamic regulation of energy expenditure [17,18].

Moreover, in the 3T3-L1 adipocyte cell line, SCD2 has been shown to be the only SCD isoform required for the differentiation of pre-adipocytes into mature adipocytes [19,20]. In these cells, SCD2 regulates the expression of the lipogenic transcription factor and master regulator of adipocyte differentiation, peroxisome proliferator-activated receptor gamma (PPARγ). Additionally, in mature adipocytes, SCD2 maintains PPARγ and PPARγ regulated gene expression [19]. In adult mice, white adipose tissue expression of SCD2 but not SCD1 is highly increased when fed a HFD or HCD [8,19].

Previously, we determined that global deficiency of *Scd2* in mice (SCD2KO) results in 100% embryonic lethality in the C57BL/6 genetic background and >70% lethality in the 129/Sv genetic background [21]. In the 129/Sv background, mice are born in typical Medelian distribution from heterozygote intercrosses. Until now, no studies have been conducted using SCD2KO mice that survived to adulthood.

Here, we investigated if whole body deletion of *Scd2* in 129/Sv mice ultimately protects lean mice from developing diet-induced adiposity during long-term consumption of either high-fat diet (HFD) or high-carbohydrate diet (HCD). To do this, we placed SCD2KO mice on HFD for 10 weeks or HCD for 6 weeks and monitored metabolic parameters. We report that global deletion of *Scd2* protects mice from diet-induced adiposity similar to global deletion of *Scd1*. SCD2KO mice failed to gain weight, had decreased % fat mass, remained glucose and insulin tolerant, and had increased markers for thermogenesis.

2. Materials and methods

2.1. Animals and diets

All animal studies were approved by and carried out in accordance with the Institutional Animal Care and Use Committee guidelines at The University of Wisconsin-Madison (protocol # A005125). Generation and maintenance of $Scd2^{-/-}$ mice have been described previously [17]. All mice used in this study were in the 129/Sv genetic background and maintained on a 12-h light/dark cycle with free access to food and water. Breeder mice were fed breeder chow (Purina 5015). Mice were weaned at 21 days post birth and fed normal chow (Purina 5008). At 6 weeks of age male and female mice were individually caged and fed either a lard-based, high-fat diet (HFD; 60% kcal from fat; Research Diets #D12492) or high-sucrose very-low-fat diet (HCD; Harlan Teklad TD.03045). Before being euthanized by isoflurane overdose, all mice were fasted for 4 h.

2.2. Quantitative real-time PCR

Total RNA was isolated using RNeasy Lipid Tissue Mini Kit (Qiagen). cDNA was synthesized from RNA using High Capacity cDNA Reverse Transcription Kit (Applied Biosystems). Quantitative reverse-transcriptase PCR (qPCR) was performed on an ABI7500 instrument using Fast SYBR Green Master Mix (Applied Biosystems). Relative mRNA abundance was calculated as relative Ct value and normalized to 18s by the   Ct: method. Primer sequences are available upon request.

2.3. Dual-energy x-ray absorptiometry (DEXA)

DEXA was performed with PIXImus software version 2.10 (GE/Lunar Corp, Madison, WI) to obtain % fat mass. Mice were anesthetized with isoflurane via an anesthesia machine (IsoFlo, Abbott Laboratories, North Chicago, IL) and placed prone with limbs and tail stretched away from the body. The analysis of each scan excluded the head.

2.4. Glucose tolerance test (GTT)

Mice were fasted for 4 h and administered 20% glucose solution at 2 g/kg glucose by oral gavage. Blood samples were collected from the tail vein at 0, 15, 30, 60, and 90 min post gavage and blood glucose was measured using a glucometer and glucose test strips (One Touch Ultra, Diabetic Express).

2.5. Insulin tolerance test (ITT)

Mice were fasted for 4 h and administered human insulin (Novo Nordisk; 0.75 U/kg) by intraperitoneal injection. Blood samples were collected from the tail at 0,15, 30, 45, 60 min post injection and blood glucose was measured using a glucometer and glucose test strips (One Touch Ultra, Diabetic Express).

2.6. Lipid analysis

Liver and adipose TG content was measured using a colorimetric biochemical assay (Wako Chemicals USA). Brain and fecal lipids were extracted using a modified Folch method and analyzed by gas-liquid chromatography (Agilent 6890) as previously described [21].

2.7. Histology

WAT was fixed in formalin then paraffin-embedded for sectioning and staining with hematoxylin and eosin (Histology Core, UW-Madison). Adipocyte area and diameter were measured using ImageJ 1.x [22].

2.8. Energy expenditure

Mice were housed in a metabolic phenotyping system (Lab-Master modular animal monitoring system; TSE, Chesterfield, MO). Six-week-old mice were individually caged and fed normal chow for 1 week. On day 8, the mice were switched to HFD for 4 days. Data collection and analysis were performed as previously reported [23].

3. Results

To determine if SCD2 deficiency protects mice from HFD induced adiposity, 6 week old male SCD2KO and WT mice were placed on HFD for 10 weeks. Similarly, to determine if SCD2 deficiency protects mice from HCD induced adiposity, 6 week old female SCD2KO and WT mice were placed on HCD for 6 weeks. Throughout both feeding studies SCD2 KO mice weighed less than the WT mice (Fig. 1A and 1B). After 10 weeks of HFD feeding, there was no difference in body weight between the average SCD2KO mice fed HFD and the SCD2KO mice fed chow (Fig. 1C). In addition, SCD2KO mice fed HCD weighed less compared to SCD2KO mice fed NC (Fig. 1D). This indicates that global deletion of *Scd2* protects mice from both HFD and HCD induced weight gain.

In accordance with their lean phenotype, SCD2KO mice fed HFD had improved glucose (Fig. 1E) and insulin tolerance (Fig. 1F) compared to WT. When given either a bolus of dextrose or insulin SCD2KO mice were able to clear blood glucose faster than WT. The initial fasted blood glucose levels were not significantly different between the genotypes.

To investigate if decreased weight gain in SCD2KO mice was due to decreased fat mass we analyzed the HFD fed mice using DEXA during the last week of the feeding study. The SCD2KO mice have a significantly lower % fat mass than the WT mice (Fig. 2A). To confirm this, tissues were dissected from the mice and weighed. The relative subcutaneous and visceral fat pad mass of SCD2KO mice fed HFD were significantly decreased compared to the WT controls (Fig. 2B). The relative subcutaneous fat pad mass of SCD2KO HCD fed mice was also decreased (Fig. 2C). Surprisingly, the relative liver mass of the HFD fed SCD2KO mice was increased (Fig. 2B). However, this was not due to an increase in TG content (Fig. 2D). The relative liver mass of HCD fed mice was similar between the genotypes (Fig. 2C). In addition, the total TG content of the subcutaneous WAT was significantly decreased in the SCD2KO mice fed HFD compared to WT mice fed HFD (Fig. 2D). Lastly, when analyzing the subcutaneous fat pad sections by light microscopy we observed that the SCD2KO fed HFD mice have smaller adipocytes compared to WT mice (Fig. 2E). The average adipocyte area and diameter are decreased in the SCD2KO mice versus the WT mice (Fig. 2F & 2G).

The protection against HFD or HCD in the SCD2KO mice is not due to decreased food intake or lack of fat absorption. Due to their size, the SCD2KO mice consumed less food

than the WT on both diets (Fig. 3A and 3C). However, once corrected for body weight, there is no difference in food consumption between SCD2KO mice and WT on HFD or HCD (Fig. 3B and 3D). Lastly, the fecal FFA content was not changed between the SCD2KO and WT mice fed HFD indicating that a difference in dietary fat absorption is notresponsible for adiposity protection (Fig. 3E).

To assess any changes in metabolic homeostasis, indirect calorimetry was performed on a cohort of 4 SCD2KO and 4 WT mice. During the first week mice consumed NC and on day 8 they were switched to HFD for 4 days. One SCD2KO mouse continuously lost weight during the first week and was excluded from the study. Overall, the SCD2KO mice consumed less oxygen than WT on both NC and HFD (Fig. 4A). Once corrected for body weight we found no significant difference in relative oxygen consumption (Fig. 4B). However, the relative expression of UCP1 and transcriptional coactivator peroxisome proliferator-activated receptor gamma, coactivator 1 alpha (PGC-1α) were increased in the brown adipose tissue of SCD2KO mice fed HFD compared to their WT counterparts (Fig. 4E). In BAT, PGC-1α regulates adaptive thermogenesis by promoting fuel uptake and energy dissipation via UPC1 [24,25]. Moreover, in support of our findings in Fig. 1A, the WT mice in the metabolic chamber began to gain weight when switched from NC to HFD while the SCD2KO mice did not (Fig. 4C). The respiratory exchange ratio between the WT and SCD2KO mice remained similar throughout the study suggesting that the SCD2KO mice did not have a systemic change in metabolism that could lead to the observed lean phenotype (Fig. 4D).

Lastly, since SCD2 is highly expressed in the brain we sought to determine if *Scd2* deficiency alters brain lipid composition. Previous reports showed that brain MUFAs regulate hepatic gluconeogenesis, food intake, insulin signaling, and adiposity [7,26]. In the SCD2KO mice, the MUFAs palmitoleic acid (16:1n7) and vaccenic acid (18:1n7) were significantly decreased in the FFA lipid class (Fig. 4F). In the TG fraction, there was an increase in 16:1n7 and decreased 16:0 (Fig. 4G). We did not observe any significant changes in the lipid profiles of DAG, CE, or PL (Fig. 4H–J).

4.   Discussion

The importance of SCD1 has been well established in metabolism and whole body energy homeostasis. Given that SCD1 and SCD2 share similar sequences and catalyze the same reaction, it is logical to assume that deletion of *Scd2* could affect energy homeostasis in a similar manner and ultimately protect mice from diet-induced adiposity. In this study, we subjected SCD2KO mice to a long-term feeding of either HFD or HCD. Generating sufficient numbers of mice for this study was a challenge and limitation because <25% of SCD2KO mice survived the first 24 h after birth. In the mice that survived, global deficiency of *Scd2* provided protection against both HFD and HCD induced adiposity due to decreased adipose tissue mass. Since we did not observe changes in food consumption or fat absorption, we hypothesized energy expenditure may be altered.

Previously, antisense oligonucleotide (ASO) mediated hypothalamic knockdown of SCD2 was reported to increase energy expenditure and blunt weight gain in obese Swiss mice [18].

Contrary to this, we did not observe a significant increase in relative oxygen consumption in mice fed HFD. However, there was a non-significant increase in relative oxygen consumption during the light cycle ($p = 0.16$) and the thermogenic markers UCP1 and PGC-1α were significantly increased in BAT. Due to our limited sample size and differences in body weight, we cannot definitively conclude that thermogenesis is increased in the SCD2KO mice.

When comparing the relative oxygen consumption of adult SCD2KO mice to reported values from adult SCD1KO mice, it is clear SCD1KO mice expend vastly greater amounts of energy [12]. One reason that accounts for this difference is the SCD1KO mice have a deleterious skin phenotype that leads to the breakdown of adaptive thermoregulation and cold intolerance [9]. SCD1KO mice are cold-sensitive which causes a robust induction of UCP1. In contrast to the SCD1KO mice, adult SCD2KO mice display a normal skin phenotype.

Furthermore, we show that *Scd2* deficiency alters brain lipid composition. Two MUFAs, palmitoleic acid (16:1n7) and vaccenic acid (18:1n7) are decreased in the brains of HFD fed SCD2KO mice. 16:1n7 is a direct product of SCD2 and can be elongated to form 18:1n7 by Elongase-6 (ELOVL6) [27]. Free MUFAs are known to signal in the hypothalamus to regulate food intake, inflammation, and hepatic glucose production [7,26]. Therefore, it is possible that the hypothalamic MUFAs 16:1n7 or 18:1n7 are acting as signaling molecules to regulate energy homeostasis. Although not significant, there was also a trend for decreased 18:1n9 in brain FFAs. The lipid composition of brain DAG, CE, and PL remained relatively unchanged. Surprisingly, there was increased 16:1n7 and a trend for increased 18:1n9 in the TG fraction.

Lastly, we provide evidence that SCD2 promotes adiposity in response to excess nutrient consumption. Although it has not been tested, we hypothesize that adipose deficiency of *Scd2* provides protection against adiposity by reducing TG synthesis in WAT and increasing thermogenesis in BAT. This could occur through deceased adipose specific MUFA synthesis or through brain-adipose crosstalk. Future experiments using tissue specific knock out mice can help dissociate the role of SCD2 in adipose and brain.

In conclusion, it is clear that SCD2 is a major player in many biological processes ranging from development to metabolism. Here, we report that global deletion of *Scd2* protects surviving mice from HFD and HCD induced adiposity. Building upon this work by using inducible SCD2-deletion models may lead to new treatments for obesity in humans. Currently, drugs targeting SCD1 can lead to dry skin and alopecia [28]. However, these side effects were not observed in adult SCD2KO mice. Perhaps drugs targeting hSCD5, which is expressed in a similar manner to SCD2, can attenuate diet-induced adiposity and related diseases in humans without causing the negative side effects observed by targeting SCD1.

Acknowledgements

References

[1]. Ravussin E, Ryan DH, Three new perspectives on the perfect storm: what's behind the obesity epidemic? Obesity 26 (1) (2018) 9–10. [PubMed: 29265770]

[2]. Miyazaki M, Bruggink SM, Ntambi JM, Identification of mouse palmitoyl-coenzyme A Delta9-desaturase, J. Lipid Res 47 (4) (2006) 700–704. [PubMed: 16443825]

[3]. Zhang S, Yang Y, Shi Y, Characterization of human SCD2, an oligomeric desaturase with improved stability and enzyme activity by cross-linking in intact cells, Biochem. J 388 (Pt 1) (2005) 135–142. [PubMed: 15610069]

[4]. Man WC, Miyazaki M, Chu K, Ntambi JM, Membrane topology of mouse stearoyl-CoA desaturase 1, J. Biol. Chem 281 (2) (2006) 1251–1260. [PubMed: 16275639]

[5]. ALJohani AM, Syed DN, Ntambi JM, Insights into stearoyl-CoA desaturase-1 regulation of systemic metabolism, Trends Endocrinol. Metabol 28 (12) (2017) 831–842.

[6]. Cao H, Gerhold K, Mayers JR, Wiest MM, Watkins SM, Hotamisligil GS, Identification of a lipokine, a lipid hormone linking adipose tissue to systemic metabolism, Cell 134 (6) (2008) 933–944. [PubMed: 18805087]

[7]. Obici S, Feng Z, Morgan K, Stein D, Karkanias G, Rossetti L, Central administration of oleic acid inhibits glucose production and food intake, Diabetes 51 (2) (2002) 271–275. [PubMed: 11812732]

[8]. Kaestner KH, Ntambi JM, Kelly TJ, Lane MD, Differentiation-induced gene expression in 3T3-L1 preadipocytes. A second differentially expressed gene encoding stearoyl-CoA desaturase, J. Biol. Chem 264 (25) (1989) 14755–14761. [PubMed: 2570068]

[9]. Lee SH, Dobrzyn A, Dobrzyn P, Rahman SM, Miyazaki M, Ntambi JM, Lack of stearoyl-CoA desaturase 1 upregulates basal thermogenesis but causes hypothermia in a cold environment, J. Lipid Res 45 (9) (2004) 1674–1682. [PubMed: 15210843]

[10]. Miyazaki M, Jacobson MJ, Man WC, Cohen P, Asilmaz E, Friedman JM, et al., Identification and characterization of murine SCD4, a novel heart-specific stearoyl-CoA desaturase isoform regulated by leptin and dietary factors, J. Biol. Chem 278 (36) (2003) 33904–33911. [PubMed: 12815040]

[11]. Wang J, Yu L, Schmidt RE, Su C, Huang X, Gould K, et al., Characterization of HSCD5, a novel human stearoyl-CoA desaturase unique to primates, Biochem. Biophys. Res. Commun 332 (3) (2005) 735–742. [PubMed: 15907797]

[12]. Ntambi JM, Miyazaki M, Stoehr JP, Lan H, Kendziorski CM, Yandell BS, et al., Loss of stearoyl-CoA desaturase-1 function protects mice against adiposity, Proc. Natl. Acad. Sci. U. S. A 99 (17) (2002) 11482–11486. [PubMed: 12177411]

[13]. Sampath H, Flowers MT, Liu X, Paton CM, Sullivan R, Chu K, et al., Skin-specific deletion of stearoyl-CoA desaturase-1 alters skin lipid composition and protects mice from high fat diet-induced obesity, J. Biol. Chem 284 (30) (2009) 19961–19973. [PubMed: 19429677]

[14]. Uto Y, Recent progress in the discovery and development of stearoyl CoA desaturase inhibitors, Chem. Phys. Lipids 197 (2016) 3–12. [PubMed: 26344107]

[15]. Tracz-Gaszewska Z, Dobrzyn P, Stearoyl-CoA desaturase 1 as a therapeutic target for the treatment of cancer, Cancers 11 (7) (2019).

[16]. Vincent BM, Tardiff DF, Piotrowski JS, Aron R, Lucas MC, Chung CY, et al., Inhibiting stearoyl-CoA desaturase ameliorates a-synuclein cytotoxicity, Cell Rep 25 (10) (2018) 2742–2754, e31. [PubMed: 30517862]

[17]. Miyazaki M, Dobrzyn A, Elias PM, Ntambi JM, Stearoyl-CoA desaturase-2 gene expression is required for lipid synthesis during early skin and liver development, Proc. Natl. Acad. Sci. U. S. A 102 (35) (2005) 12501–12506. [PubMed: 16118274]

[18]. de Moura RF, Nascimento LF, Ignacio-Souza LM, Morari J, Razolli DS, Solon C, et al., Hypothalamic stearoyl-CoA desaturase-2 (SCD2) controls whole-body energy expenditure, Int. J. Obes 40 (3) (2016) 471–478.

[19]. Christianson JL, Nicoloro S, Straubhaar J, Czech MP, Stearoyl-CoA desaturase 2 is required for peroxisome proliferator-activated receptor gamma expression and adipogenesis in cultured 3T3-L1 cells, J. Biol. Chem 283 (5) (2008) 2906–2916. [PubMed: 18032385]

[20]. Cantley JL, O'Neill LM, Ntambi JM, Czech MP, The cellular function of stearoyl-CoA desaturase-2 in development and differentiation, in: Ntambi PDJM (Ed.), Stearoyl-CoA Desaturase Genes in Lipid Metabolism, Springer New York, New York, NY, 2013, pp. 119–130.

[21]. Flowers MT, Ade L, Strable MS, Ntambi JM, Combined deletion of SCD1 from adipose tissue and liver does not protect mice from obesity, J. Lipid Res 53 (8) (2012) 1646–1653. [PubMed: 22669918]

[22]. Schneider CA, Rasband WS, Eliceiri KW, NIH Image to ImageJ: 25 years of image analysis, Nat. Methods 9 (7) (2012) 671–675. [PubMed: 22930834]

[23]. Banh T, Nelson DW, Gao Y, Huang TN, Yen MI, Yen CL, Adult-onset deficiency of acyl CoA:monoacylglycerol acyltransferase 2 protects mice from diet-induced obesity and glucose intolerance, J. Lipid Res 56 (2) (2015) 379–389. [PubMed: 25535286]

[24]. Liu C, Lin JD, PGC-1 coactivators in the control of energy metabolism, Acta Biochim. Biophys. Sin 43 (4) (2011) 248–257. [PubMed: 21325336]

[25]. Puigserver P, Wu Z, Park CW, Graves R, Wright M, Spiegelman BM, A cold-inducible coactivator of nuclear receptors linked to adaptive thermogenesis, Cell 92 (6) (1998) 829–839. [PubMed: 9529258]

[26]. Cintra DE, Ropelle ER, Moraes JC, Pauli JR, Morari J, Souza CT, et al., Unsaturated fatty acids revert diet-induced hypothalamic inflammation in obesity, PloS One 7 (1) (2012), e30571. [PubMed: 22279596]

[27]. Jakobsson A, Westerberg R, Jacobsson A, Fatty acid elongases in mammals: their regulation and roles in metabolism, Prog. Lipid Res 45 (3) (2006) 237–249. [PubMed: 16564093]

[28]. Theodoropoulos PC, Gonzales SS, Winterton SE, Rodriguez-Navas C, McKnight JS, Morlock LK et al., Discovery of tumor-specific irreversible inhibitors of stearoyl CoA desaturase, Nat. Chem. Biol 12 (4) (2016) 218–225. [PubMed: 26829472]
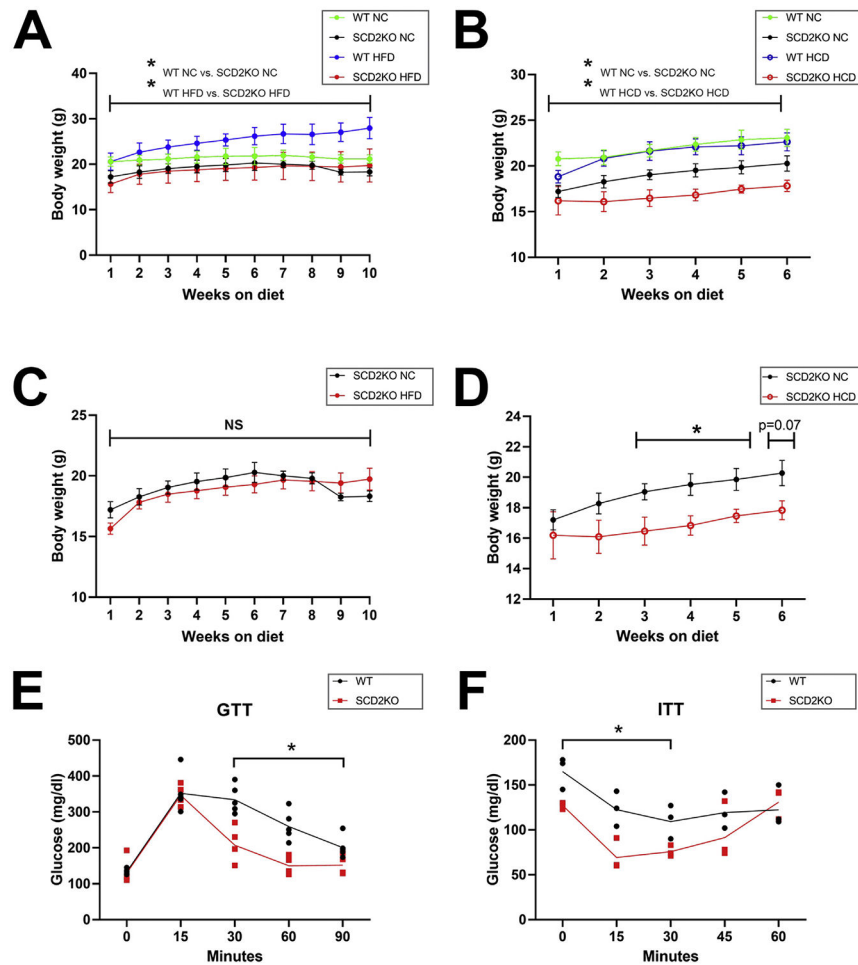
Fig. 1. Body weight, GTT, and ITT

(A) Weekly body weight of male WT and SCD2KO mice fed either NC or HFD (n = 6 WT NC, 4 SCD2KO NC, 9 WT HFD, 16 SCD2KO HFD). (B) Weekly body weight of female WT and SCD2KO fed either NC or HCD (n = 3 WT NC, 3 SCD2KO NC, 3 WT HCD, 4 SCD2KO HCD (C) Weekly body weight of WT vs. SCD2KO mice fed HFD. (D) Weekly body weight of WT vs. SCD2KO mice fed HCD. (E) GTT of 12–15 week old male WT and SCD2KO mice fed HFD (n = 4). (F) ITT of 12–15 week old male WT and SCD2KO mice fed HFD (n = 3). Values are mean ± SEM, ns = not significant, *P < 0.05 vs. WT by Student's two-tailed *t*-test.
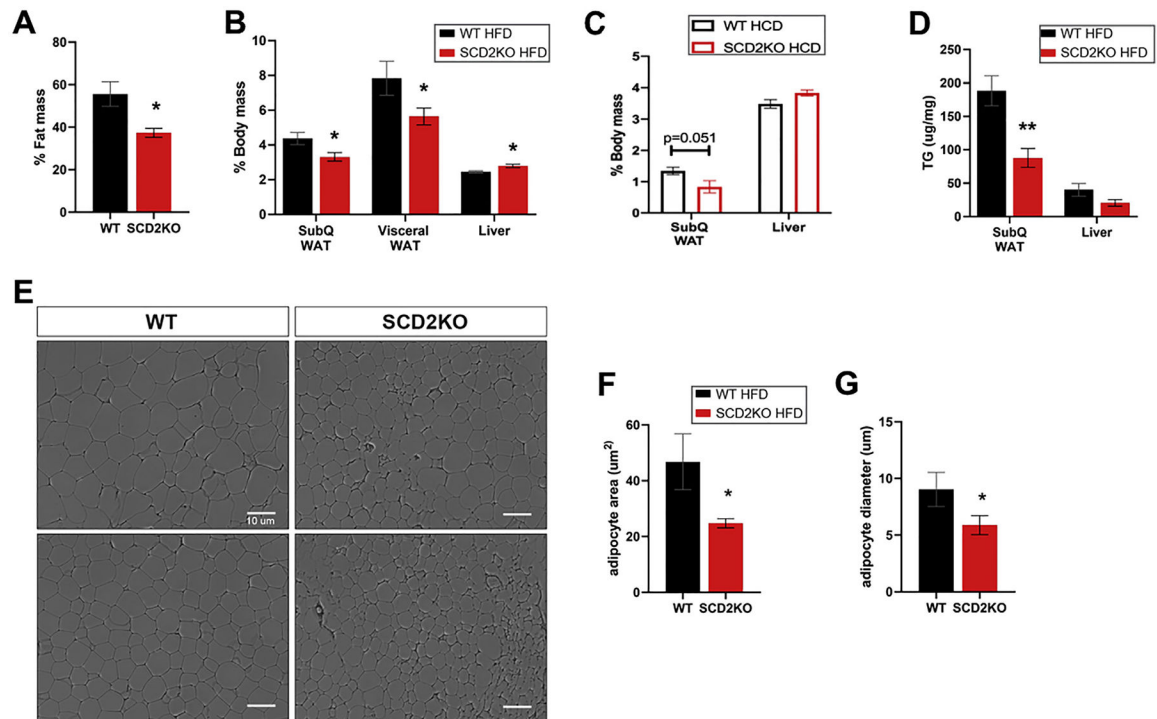
Fig. 2. Adipose mass and size

(A) % Fat mass, measured by DEXA, of 15 week old male WT (n = 5) and SCD2KO mice (n = 7) fed HFD. (B) Subcutaneous WAT, visceral WAT, and liver % body mass of 15 week old male WT (n = 9) and SCD2KO mice (n = 16) fed HFD. (C) Subcutaneous WAT and liver % body mass of 12 week old female WT (n = 3) and SCD2KO mice (n = 4) fed HCD. (D) Subcutaneous WAT and liver TG content of 15 week old male WT (n = 5) and SCD2KO (n = 4) mice fed HFD. (E) H&E stained subcutaneous WAT sections of WT and SCD2KO mice fed HFD. (F) Average adipocyte area (n = 3 WT, 3 SCD2KO; >1000 cells). (G) Average adipocyte diameter (n = 3 WT, 3 SCD2KO; >1000 cells). Values are mean ± SEM, *P < 0.05, **P < 0.01 vs. WT by Student's two-tailed *t*-test.
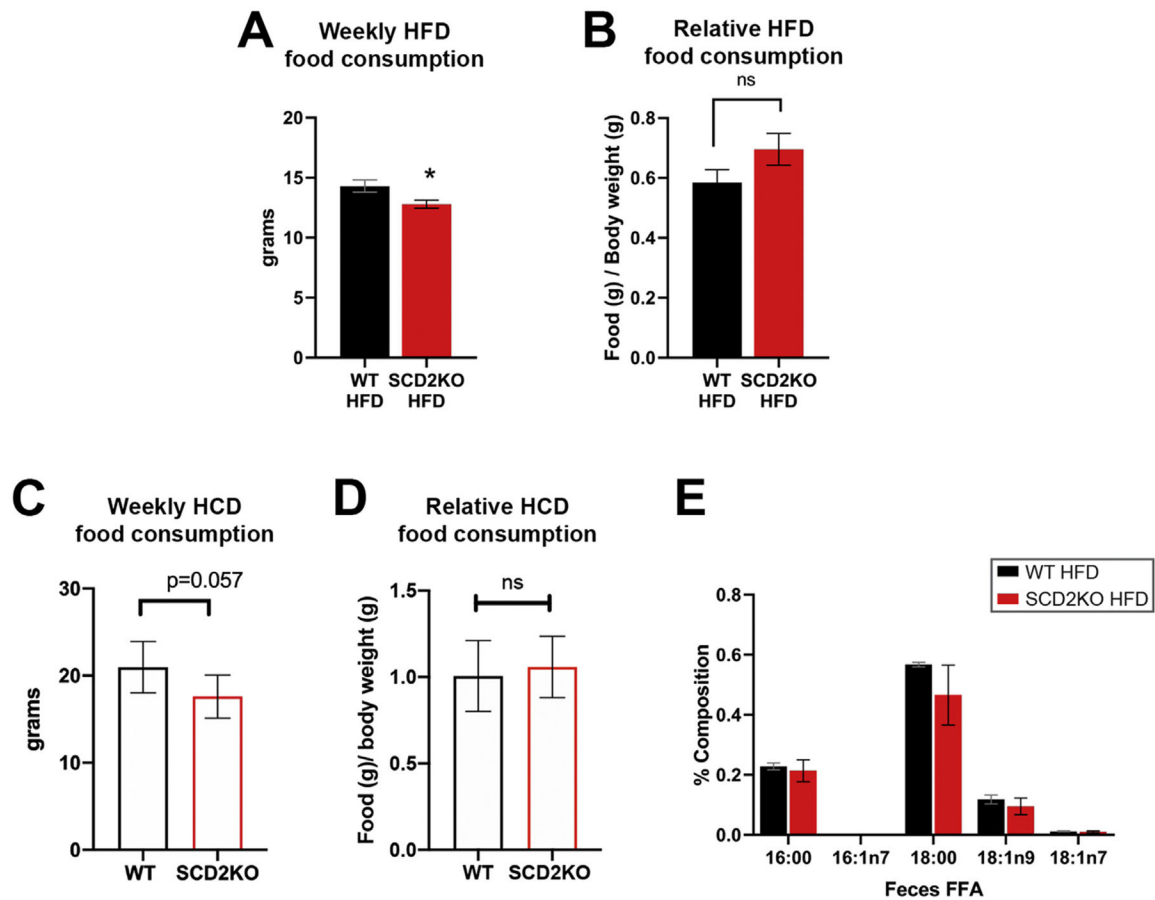
Fig. 3. Food consumption and absorption
(A) Average weekly HFD food consumption of male WT (n = 9) and SCD2KO (n = 16) mice. (B) Average weekly HFD food consumption of male WT (n = 9) and SCD2KO (n = 16) mice relative to body weight. (C) Average weekly HCD food consumption of female WT (n = 3) and SCD2KO (n = 4) mice. (D) Average weekly HCD food consumption of female WT (n = 3) and SCD2KO (n = 4) mice relative to body weight. (E) Fecal FFA % composition of male WT (n = 4) and SCD2KO (n = 4) mice fed HFD. Values are mean ± SEM, ns = not significant, *P < 0.05 vs. WT by Student's two-tailed *t*-test.
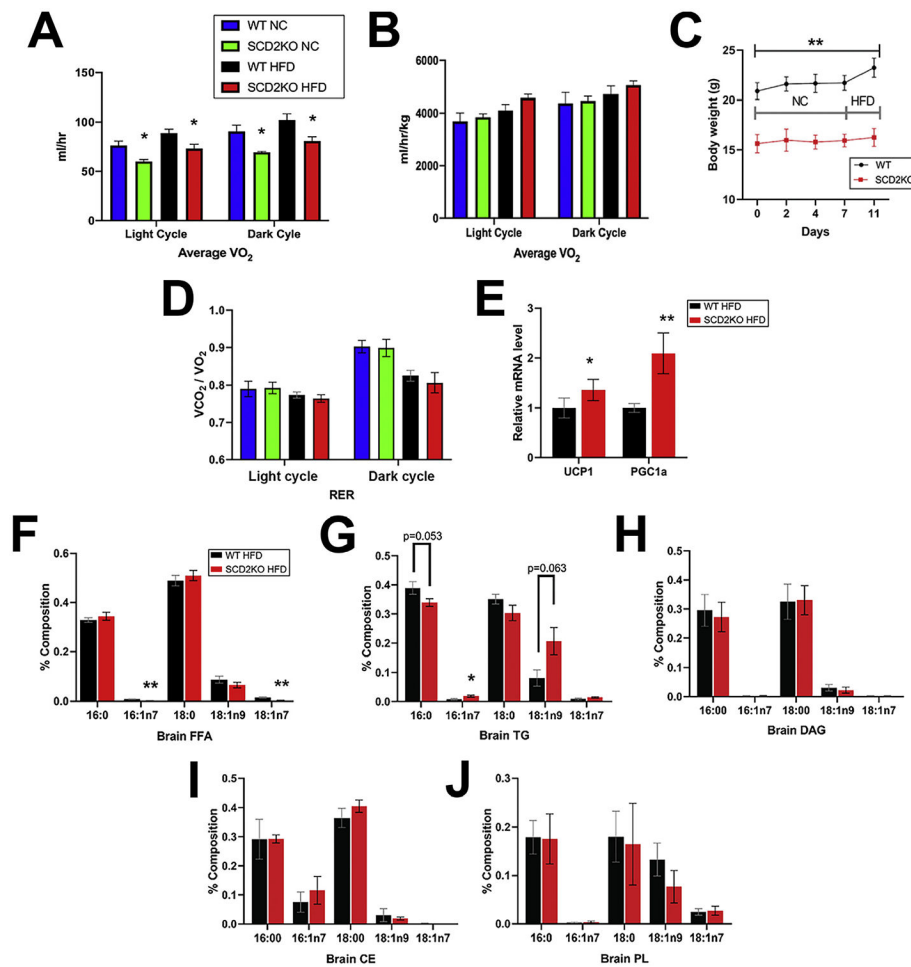
Fig. 4. Energy expenditure and brain lipid composition

(A) Average oxygen consumption of 6 week old male WT and SCD2KO mice fed NC and HFD (n = 4 WT, 3 SCD2KO). (B) Average oxygen consumption relative to body weight of 6 week old male WT and SCD2KO mice fed NC and HFD (n = 4 WT, 3 SCD2KO). (C) Daily body weight of 6 week old male WT (n = 4) and SCD2KO (n = 3) mice fed NC for 7 days and switched to HFD for 4 days. (D) RER of 6 week old male WT and SCD2KO mice fed NC and HFD (n = 4 WT, 3 SCD2KO). (E) Relative gene expression of UCP1 and PGC-1α in BAT of 15 week old WT (n = 4) and SCD2KO (n = 4) mice fed HFD. (F) % Composition of brain FFAs from male WT (n = 5) and SCD2KO (n = 5) mice fed HFD. (G) % Composition brain TG from HFD fed WT (n = 5) and SCD2KO (n = 5) mice. (H) % Composition brain DAG from HFD fed WT (n = 5) and SCD2KO (n = 5) mice (I) % Composition brain CE from HFD fed WT (n = 5) and SCD2KO (n = 5) mice (J) % Composition brain PL from HFD fed WT (n = 5) and SCD2KO (n = 5) mice. Values are mean ± SEM, *P < 0.05 vs. WT by Student's two-tailed *t*-test. Values are mean ± SEM, *P < 0.05, **P < 0.01 vs. WT by Student's two-tailed *t*-test.